Bioavailability of Octamethylcyclotetrasiloxane (D_4) After Exposure to Silicones by Inhalation and Implantation

Hoan-My Do Luu and Joseph C. Hutter

Center for Devices and Radiological Health, U.S. Food and Drug Administration, Rockville, Maryland, USA

We developed a physiologically based pharmacokinetic (PBPK) model to predict the target organ doses of octamethylcyclotetrasiloxane (D_4) after intravenous (IV), inhalation, or implantation exposures. The model used ^{14}C-D_4 IV disposition data in rats to estimate tissue distribution coefficients, metabolism, and excretion parameters. We validated the model by comparing the predicted blood and tissues concentrations of D_4 after inhalation to experimental results in both rats and humans. We then used the model to simulate D_4 kinetics after single and/or repeated D_4 exposures in rats and humans. The model predicted bioaccumulation of D_4 in fatty tissues (e.g., breast), especially in women. Because of its high lipid solubility (Log $P_{oct/water}$ = 5.1), D_4 persisted in fat with a half life of 11.1 days after inhalation and 18.2 days after breast implant exposure. Metabolism and excretion remained constant with repeated exposures, larger doses, and/or different routes of exposure. The accumulation of D_4 in fatty tissues should play an important role in the risk assessment of D_4 especially in women exposed daily to multiple personal care products and silicone breast implants. *Key words*: bioavailability, breast implant, D_4, implantation, inhalation, octamethylcyclotetrasiloxane, PBPK, physiologically based pharmacokinetic model, risk assessment, silicone. *Environ Health Perspect* 109:1095–1101 (2001). [Online 11 October 2001] *http://ehpnet1.niehs.nih.gov/docs/2001/109p1095-1101luu/abstract.html*

Octamethylcyclotetrasiloxane or D_4 (CAS #556-67-2) is a low molecular weight siloxane (LMWS) fluid with a low surface tension, low aqueous solubility, high lipid solubility, and low vapor pressure (Figure 1, Table 1). It is present at 40–60% by weight in personal care products such as antiperspirants, cosmetics, and hair care products (*2–4*). Because of its widespread use in these products, a typical woman is exposed to an average daily intake (ADI) of 0.158 mg/kg/day (11.1 mg/day) of D_4 from daily use of such products (*4*).

D_4 is also used to manufacture polydimethylsiloxane (PDMS) polymer. PDMS is commonly used in orthopedic and breast implants (*5*). Although breast implants are composed mostly of stable high molecular weight siloxanes (HMWS), low molecular weight siloxanes (LMWS) still exist in the polymer as impurities (*5–9*). LMWS consist of both cyclic and linear molecules with repeating units of dimethylsiloxane, of which D_4 is a major component (47%) (*7–9*). Residual LMWS ranged from 0.2 to 2% by weight for the silicone gel and 0.01% to 0.1% for the silicone envelope (1.04–10.4 mg) (*5–9*). Numerous studies have documented the migration of significant amounts of LMWS out of breast implants into surrounding breast tissues and to the liver (*8–11*). This would add to the dermal or inhalation exposures from personal care products in a typical woman.

The disposition of [^{14}C]D_4 in mice and rats revealed wide tissue distributions after intravenous (IV), subcutaneous, and inhalation exposures, respectively (*1,12–14*). Female rats exposed to D_4 via inhalation induced more liver metabolizing enzymes such as cytochrome P_{450} (CYP) and retained higher amounts of D_4 than did male rats (*1,12,15*). CYP is a family of enzymes that play a major role in the oxidative and reductive metabolism of many drugs, many xenobiotics, and steroids. Two major and three minor metabolites of D_4 have recently been identified in rat urine (*16*). At high doses, mice and rats had enlarged lungs and liver as well as developmental effects such as decreased live litter size, number of pups, and number of uterine implantation sites (*1,4,12,13,15*). There is little information concerning the effects of the highly lipid soluble D_4 in humans, but it is not expected to be inert if it accumulates in the body (*9–12*).

Previously, Andersen et al. (*16*) used physiologically based pharmacokinetic (PBPK) modeling to determine D_4 disposition in Fisher 344 rats after inhalation doses (*16*). Although the model provided a reasonable simulation of the disposition of D_4 during exposure, it underestimated the postexposure levels of D_4 experimentally found in blood and tissues. It failed to account for the gradual rate of decline of D_4 exhalation in rats after exposure, and the authors reported no extrapolation to human exposure (*16*).

A goal of this study was to develop a validated PBPK model to relate external exposure of D_4 to internal target dose (bioavailability) in women with silicone breast implants. The model was first calibrated using previously reported data on tissue distribution in female rats after single and repeated IV administrations of ^{14}C-D_4 (*1*). We validated the predicted results in rats and in humans after inhalation exposure using published independent data (*12,17,18*). We then used the validated model to predict the pharmacokinetics of D_4 as leached from saline-filled breast implants in women.

Methods

PBPK model. The PBPK model (Figure 2) uses the actual physicochemical properties of D_4 and physiologic measurements of animals or humans as a basis for calculating the disposition of D_4. Material balances were written for D_4 for each of the model's compartments: lungs, blood, two fat compartments, richly perfused tissues, gastrointestinal tract, kidneys, and liver (see Appendix for details). This model was based on a previously published PBPK model for styrene (*19*) and 4,4′-methylenedianiline (MDA) (*20*).

In this model, D_4 was metabolized in the liver, and all the metabolites were excreted in the urine or feces (*1,12*). Generally lipids are transported in blood by various lipoproteins such as low-density lipoproteins (LDL), high-density lipoproteins (HDL), and chylomicrons (*22*). The highly lipid-soluble D_4 is likely to be transported in blood by one or more of these carriers. We found it necessary for D_4 to be bound to two lipoproteins of different binding affinities (weakly bound

Address correspondence to H-M. D. Luu, U.S. FDA, Center for Devices and Radiological Health, 12725 Twinbrook Parkway HFZ-150, Rockville, MD 20852 USA. Telephone: (301) 827-4711. Fax: (301) 827-4853. E-mail: hml@cdrh.fda.gov

We thank R. Kammula, M. Myers, C.S. Kim, and L. Schroeder for helpful suggestions in this investigation. Without their help, this study would not have been possible.

This work was presented in part at the 219th Annual Meeting of the American Chemical Society, April 2000, Anaheim, CA.

The opinions or assertions about specific products identified by brand name herein are the private views of the authors and are not to be construed as conveying either an official endorsement or criticism by the U.S. Department of Health and Human Services or the Food and Drug Administration.

Received 23 March 2001; accepted 5 April 2001.

and strongly bound) to account for D_4 kinetics in blood (*1,12*). Physiologic values (e.g., blood flows; tissue and organ volumes) in the model were taken from the literature (Table 2). We adjusted other parameters needed to calibrate the model—such as tissue distribution coefficients, metabolism and excretion parameters, and the blood:air distribution coefficient (H_{air}, reciprocal of Henry's Law constant)—to fit the experimentally determined tissue distribution

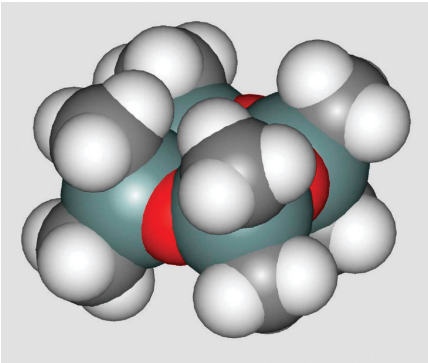

Figure 1. Three-dimensional structure of D_4. Unique chemical properties were caused by methyl groups (white), which shield the oxygen atom (red) and reduced the polarizability of the molecule.

Table 1. Physical properties of D_4.

Property	Measures
Molecular weight	296.62
Vapor pressure	1 mm Hg at 25°C
Boiling point	175.4°C
Surface tension	18.796 dynes/cm
Aqueous solubility	56 ppb
Viscosity	2.3 cp at 25°C
Melting point	17.5°C
Log $P_{octanol:water}$	5.1

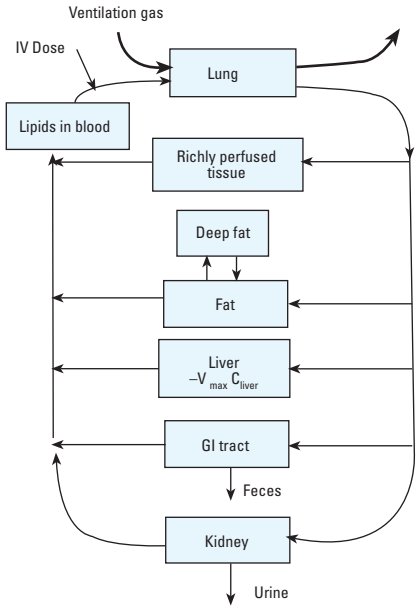

Figure 2. Flow diagram for the PBPK model.

plasma as reported by Kirkpatrick et al. (*1*). We solved the equations using an adaptive grid Runge-Kutta method (Mathcad 8.0; MathSoft, Inc., Cambridge, MA, USA). The solutions to these multiple stiff ordinary differential equations describe the time course of D_4 in the rat. The model predicts the time course of D_4 at target tissues, as well as excretion rates, and the variation of these responses as a function of the dose, duration, and route of exposure. Once we obtained the best fit for the rat IV experiments, the model parameters were scaled up to the known human physiology based on power law ($Y = a\ M^{3/4}$) (*23*). The model was validated in both the rat and human by independent prediction and comparison to inhalation results in both rat and human (*12,17*).

Model calibration. We calibrated the PBPK model using blood/tissues distribution data by Kirkpatrick et al. (*1*). Briefly, three groups of 20 Sprague-Dawley (SD) rats (10 males and 10 females) were injected intravenously with single 7 mg/kg and 70 mg/kg and repeated 7 mg/kg daily doses of ^{14}C-D_4 for 14 days. Blood samples were taken from tail vein at predose, 10, 20, 40 min and 1, 2, 4, 6, 12, 24, 36, and 48 hr postdose from two groups of rats comprising five animals of each sex. The animals were subsequently sacrificed and the liver, kidneys, lungs, and samples of fat were taken from each animal for radioactive determination of tissue distribution of D_4. In another group of 10 rats (5 males and 5 females), D_4 was administered intravenously via tail vein at 7 mg/kg ^{14}C-D_4 as described above. These animals were placed in metabolism cages and urine, feces, and expired air were collected from each animal 0- to 6-hr, 6- to 12-hr, and subsequent 24-hr intervals for up to 5 days. The animals were sacrificed at completion and the liver, kidneys, lungs, samples of fat, gastrointestinal (GI) tract, and remainder of carcass taken for measurements of radioactivity.

Model validation. **Rat inhalation model.** We extrapolated the rat IV model to simulate rat inhalation exposure as reported by Plotzke et al. (*12*). In this study, F344 rats were exposed to 7, 70, or 700 ppm ^{14}C-D_4 by inhalation for 6 hr. Up to 168 hr after exposure, total body burden, excretion in urine, feces, exhalation, and accumulation in target tissues (liver, lungs, perirenal fat, ovaries, vagina, and testes) were measured (*12*).

Human inhalation model. We scaled the rat calibrated PBPK model to humans as described previously, and then compared the human model prediction for inhalation exposure with experimental data obtained from an independent inhalation study (*17*). In the human inhalation exposure study, Utell et al. (*17*) exposed 12 volunteers using a mouthpiece-exposure system for 1 hr to either air or 10 ppm (122 µg/L) D_4 vapor. Utell et al. (*17*) divided each exposure into three rest periods of 10, 20, and 10 min, respectively, and two exercise periods, each of 10-min duration. The order of D_4 exposure was randomized. Exhaled air samples were collected before, immediately after exposure, and at 1 and 6 hr after exposure. D_4 was extracted from plasma samples with tetrahydrofuran and the D_4 analysis was performed using gas chromatography–mass spectrometry analysis as described elsewhere (*21*).

Breast implant exposure. In our simulation, the maximum dose of residual D_4 that could migrate from silicone breast implants was estimated to be 0.1% wt of the silicone implant envelope (0.15 mg/kg or 10.4 mg) (5). The residual D_4 was left by incomplete devolatization of medical polymer (*5,7–9*).

Lykissa et al. (*9*) measured *in vitro* the diffusion rate of LMWS (D_4-D_7) from explanted silicone gel-filled breast implants into various surrounding media. The highest reported diffusion rate (40 µg/g implant/day) was for a lipid-rich medium such as that

Table 2. Values of physiologic parameters used in the models.

Parameters	Rat values	Human values
Plasma volume (V_{blood}) mL	8.5	2,800
Blood flows mL/min		
Richly perfused tissues (Q_r)	44	2,054
Fat (Q_f)	34.2	442
Liver (Q_l)	15.2	1,196
GI tract (Q_{gi})	11.6	728
Kidney (Q_k)	11.7	780
Total cardiac output mL/min (Q_t)	116.7	5,200
Lung ventilation rate (Q_{air})	93.6 mL/min	10–30 L/min
Tissue compartment volumes mL		
Lungs (V_{lung})	14	3,800
Richly perfused tissues (V_r)	146	40,672
Fat (V_f)	14.2	14,562
Liver (V_l)	8.0	1,419
GI tract (V_{gi})	6.0	948
Kidney (V_k)	1.9	243

See Appendix for nomenclature.

found in breast tissue, and the lowest reported rate was for an aqueous extraction media (< 1 µg/g implant/day). Given the *in vitro* results for D_4 into lipid rich medium, the estimated diffusivity of D_4 in the breast implant shell was 5.4×10^{-8} cm^2/sec. Using published values of the diffusivity for different compounds in PDMS and free volume theory, we also estimated the diffusivity of D_4 to be 2×10^{-8} cm^2/sec in the breast implant shell (*24,25*). Thus, the leaching rate of D_4 from the shell to the surrounding fatty tissues of the breasts was estimated to be 95% removal in 30 days. We obtained this rate by solving one-dimensional diffusion equation inside a breast implant shell (5–7 g) exposed to an infinite sink (the body) using estimated values of the diffusivity (5.4×10^{-8} cm^2/sec, 0.3 mm shell thickness) of D_4 (*26*). This conservative estimate for diffusion in a rubbery polymer allows for all of the D_4 to be removed from the breast implant shell rapidly within a month (*9*). In the actual human body, external mass transfer resistance will slow the rate down and allow the D_4 to persist in the body even longer (*27*). The dose of D_4 from silicone gel implant is expected to be higher (*9*), because the initial mass of D_4 in the silicone gel leaching out of the silicone polymer envelope (which is permeable to its own components) is higher, even years after implantation (*9–11*).

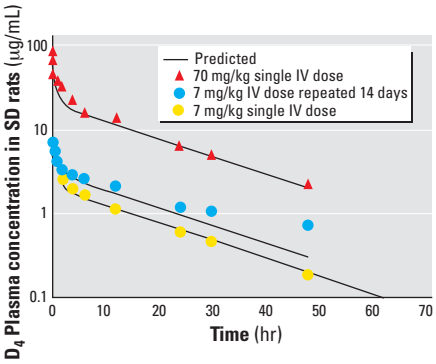

Figure 3. Predicted and experimental D_4 plasma concentrations in rats exposed by IV.

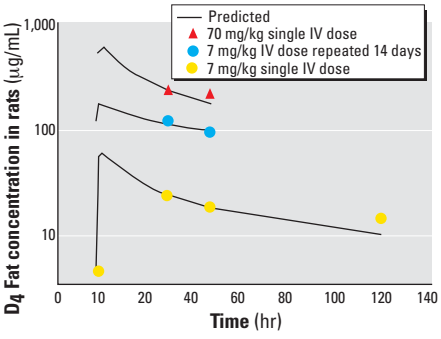

Figure 4. Predicted and experimental D_4 fat concentrations in rats exposed by IV.

Results

The predicted and experimental plasma and fat results in the SD rats are shown in Figures 3 and 4, respectively. The model parameters in the rat are shown in Table 3. The experimental data showed higher accumulation of radioactivity in female rats than in male rats at all doses (*1,12*). We used only the data from female rats to develop our model because our goal was to assess the exposure of D_4 in women.

The plasma radioactivity profiles of ^{14}C-D_4 showed nonlinear kinetics for different dosage regimens (Figure 3). Single IV dose of 7 mg/kg ^{14}C-D_4 had two half-lives ($t_{1/2}$ = 2.1 hr and 12.7 hr) and 14-day repeated daily dose of 7 mg/kg ^{14}C-D_4 had three half-lives ($t_{1/2}$ = 3.2 hr, 15.9 hr, and 32.7 hr). Table 4 shows the tissue distribution results obtained in the IV rat studies. The highest radioactivity accumulated in fat followed by richly perfused tissues (i.e., lungs, brain), blood, liver, and kidneys. Approximately 60–80% of the absorbed D_4 dose was exhaled and excreted in the urine and feces. Figure 4 shows the predicted and experimental time and dose response of ^{14}C-D_4 in fatty tissues of the treated rats.

Table 5 shows the pharmacokinetic results obtained in the IV rat studies. For the repeated doses, the exposure as defined by area under the curve (AUC = 43.4 vs. 663.3 µg hr/mL) substantially increased, but the clearance remained the same.

To validate the rat model, we compared the inhalation results obtained from the model with independent inhalation exposure data in F344 rats reported by Plotzke at al.

Table 3. Values of the parameters used in the models.

Parameters	Rat values	Human values
Deep fat parameters[a]		
Q_{f2}/Q_{f1}	0.059	0.059
V_{f2}/V_{f1}	0.73	0.73
D_4 distribution coefficients[b]		
Richly perfused tissue (D_r)	10	10
Weakly bound fat compartment (D_{f1})	700	700
Strongly bound fat compartment (D_{f2})	2,000[b,c]	2,000[b,c]
Liver (D_l)	7.4[d], 160[e]	7.4
GI tract (D_{gi})	0.41	0.41
Kidney (D_k)	40	40
Blood air partition constant, (H_{air}[a])	20.0	20.0
K_{el} h^{-1} [f,b]	9[d], 4[e]	728
Strongly bound plasma lipoproteins[a]		
V_{strong} mL[g]	1.0	0.0
K_{si} h^{-1}	0.4	–
K_{so} h^{-1}	0.07	–
Weakly bound plasma lipoproteins[a]		
V_{weak} mL[g]	1.0	10.4
K_{wi} h^{-1}	0.2	0.2
K_{wo} h^{-1}	1.0	1.0
Capture efficiency, η	0.04[e]	0.12 resting, 0.07 exercise
Initial inhalation fraction D_4 in weakly bound plasma lipoprotein, α	0.07[e]	0.008

Abbreviations: k_{el}, metabolism rate constant, per hour; k_{si}, forward rate constant for strong protein binding of D_4 in plasma, per hour; k_{so}, reverse rate constant for strong protein binding of D_4 in plasma, per hour; k_{wi}, forward rate constant for weak protein binding of D_4 in plasma, per hour; k_{wo}, reverse rate constant for weak protein binding of D_4 in plasma, per hour; Q_{f1}, blood flow rate to weakly bound fat compartment, mL/hr; Q_{f2}, blood flow rate to strongly bound fat compartment; mL/hr. See Appendix for nomenclature.
[a]Best fit parameters to experimental data. [b]Determined from distribution and excretion study in rats (1). [c]Estimated from Log P = 5.1. [d]Sprague-Dawley rat. [e]F344 rat. [f]Scale-up factor (70 kg/0.20 kg), 0.75. [g]Scale-up factor (70 kg/0.20 kg), 0.40.

Table 4. Comparison of D_4 tissue distribution results in rats as a percentage of doses. Experimental values in parentheses.

Tissue compartment	Rat IV[a] (7 mg/kg)	Rat IV[a] (70 mg/kg)	Rat IV 14-day repeated dose (7 mg/kg)
Richly perfused tissue	0.83	0.84	0.20
Fat	18.2 (16.3)	18.2 (18.8)	6.9
Liver	0.10 (0.15)	0.10	0.024
GI tract	0.001	0.001	0.0003
Kidneys	0.04 (0.07)	0.04 (0.05)	0.01
Blood	0.15	0.15	0.015
Urine	26.1 (22.3)	26.1	32.2
Feces	8.71 (5.93)	8.71	10.7
Exhaled	42.2 (31.8)	42.2	50.2

[a]At the end of 48 hr.

(*12*). The F344 rat results were obtained using higher metabolism rate than in SD rats (*12*). Also, the higher ventilation rate in the rat produced lower capture efficiency than in the human ventilation model. As in the IV rat model, the experimental inhalation results in F344 rats also indicated a biphasic plasma profile as well as slow clearance in fat, in fairly good agreement with the predictions of the model (Figure 5). These results showed less accumulation in fat compared to rat IV exposure results. After 60 hr, the simulated plasma results were below the reported experimental data, which were reported as the limit of detection (0.01 µg/g). Hence, we cannot really compare, but the model does not conflict with the experimental results. Previous rat experiments indicated rapid clearance of D_4 in plasma (*1*).

To validate the human model, we predicted the absorption, distribution, metabolism, and excretion of D_4 after an inhalation dose and compared it to previously published experimental results by Utell et al. (*17*). Figure 6 displayed the predicted and experimental profiles of D_4 after a single dose of 11.1 mg by inhalation for 1 hr in human plasma and fat, respectively. As shown, the model was an excellent predictor of the experimentally determined plasma concentrations.

Table 6 shows the simulated results for tissue distribution, exhalation, and excretion in the urine and feces for human inhalation and implantation. Table 7 shows the pharmacokinetics of D_4 in plasma. Like fat in rats, the human fat showed highest accumulation of D_4 regardless of dose, regimen, or route of exposure.

A single low-dose D_4 exposure by inhalation showed fast plasma absorption (C_{max} = 69.4 ng/mL at t_{max} = 1 hr) and fast excretion [43.8% exhaled, 6.1% in urine, 2% in feces; Clearance = 407 mL/hr (Table 7)]. Repeated daily exposure to the same low dose of D_4 for 14 days showed higher C_{max} value (76 ng/mL) at 145 hr after exposure, increased area under the curve (AUC = 3,628 ng hr/mL), increased volume of distribution (V_d = 1,022 L) and reduced systemic clearance (Clearance = 357 mL/hr). The implantation of silicone breast implants had a lower C_{max} of 2 ng/mL compared to a C_{max} of 69.4 ng/mL and 76 ng/mL after single or repeated inhalation of 11.1 mg/day for 7 days, respectively. Comparison of different routes of exposure in human showed largest volume of distribution (V_d = 4,100 L) after implantation, indicating longer retention in the body. We predicted that D_4 systemic exposure would be longer after implantation ($t_{1/2}$ = 18 days for D_4 in fat) compared to inhalation ($t_{1/2}$ = 11 days in fat). The maximum amount retained in fat for the breast implant case was 174 ng/mL at t_{max} =11.7 days after implantation compared to a corresponding C_{max} = 330 ng/mL at t_{max} = 34 hr after inhalation.

Table 5. Pharmacokinetic results of D_4 in rat plasma.

Pharmacokinetic parameters	Rat IV – single dose 7 mg/kg	Rat IV – 14 day repeated dose 7 mg/kg
C_{max} (µg/mL)	6.7	7.6
t_{max} (hr)	0	312[a]
AUC (µg/hr/mL)	43.4	663.2
Cl (mL/hr/kg)	2.42	2.46
V_d (L/kg)	1.05	0.92
$t_{1/2}$ experimental (hr)	2.1, 12.7	3.2, 15.9, 32.7
$t_{1/2}$ model (hr)	2.7, 14.0	3.4, 14.4

Abbreviations: AUC, area under the curve of D_4 concentration in plasma versus time; Cl, total body clearance; C_{max}, maximum concentration in plasma; t_{max}, maximum time; $t_{1/2}$, plasma elimination half-life of D_4; V_d, volume of distribution. See Appendix for nomenclature.
[a]Maximum concentration occurs immediately after dosing at the beginning of day 14.

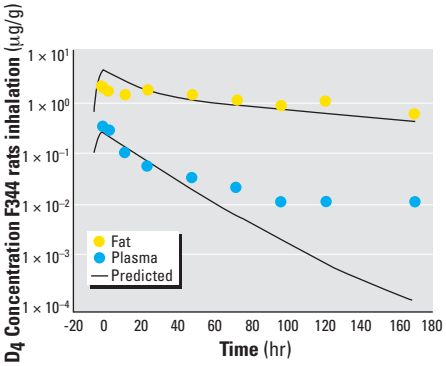

Figure 5. Predicted and experimental D_4 plasma and fat concentrations in rats exposed by inhalation. Limit of detection = 0.01 µg/g.

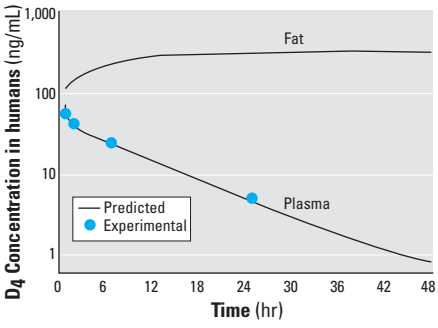

Figure 6. Predicted and experimental D_4 plasma and fat concentrations in humans exposed by inhalation.

Discussion

Women are prone to bioaccumulate D_4 when exposed daily to such multiple personal care products as antiperspirants, skin care, or hair care products. A mean dose of 0.158 mg/kg D_4 per day by inhalation was reported in a recent abstract by Shipp et al. (*4*). Added to this would be the estimated dose (10.4 mg/30 days/60 kg = 0.0057 mg/kg/day) of D_4 leached from the saline-filled silicone breast implants (*5–9*). For the first time, the results of the PBPK model suggest that women accumulate D_4 in their fatty tissues (e.g., breasts), richly perfused tissues, liver, and kidneys. The D_4 accumulation increases with the dose, the regimen of dosing (single vs. repeated), and the routes of exposure (inhalation vs. implantation).

The resulting tissue distribution is attributed to the physical properties of D_4, which is highly lipid soluble and very insoluble in water (Figure 1, Table 1). Thus, once lipid-containing tissue (e.g., breast tissue) is exposed to D_4—as occurs when D_4 leaches from breast implants—D_4 is rapidly absorbed and only slowly desorbed with a very long half-life (fat $t_{1/2}$ = 18.2 days). D_4 is retained in the body if during exposure it contacts the lipophilic tissues. Thus neither inhalation exposure (about a 10% capture of the intake dose) nor dermal contact (0.5% absorption) is an efficient way to deliver D_4 into internal target organs in the body (*17,28*). By contrast, leaching from an implant directly into breast tissue (mostly fat) would have great potential for allowing accumulation of D_4 in the body. Repeated exposures increase accumulation in target tissues since the frequency of exposure is shorter than the elimination half-life, especially in certain target tissues.

Fat is the primary tissue depot following all routes of exposure, at low and high doses of D_4, with significant longer half-life than that of plasma (Table 4 and 5). In the rat, the highest D_4 accumulation was in the fat, followed by richly perfused tissues (e.g., lungs, brain), blood, liver, and kidneys (Table 4). Single-dose inhalation results in rats were similar, with rapid clearance from plasma and a longer half-life in fat (Figure 5). The single inhalation route in rats also had poor absorption, which was consistent with both our inhalation model and published results (*12*). Predictions of the PBPK model regarding plasma, tissue distributions, and excretions were consistent with the above reported experimental results (*1,12*).

In the human inhalation case, the model predicted that the biphasic plasma half-life would be 1.7 and 7.4 hr, and the fat half-life would be 11.1 days. Similarly, the model predicted that after desorption of D_4

from the breast implant in the human, the plasma half-life would be 7.8 hr and the fat half-life would be 18.2 days (Table 7). If D_4 exposures were repeated in either case at a frequency shorter than the fat half-life, the net result would be accumulation in the fat tissues, because the input would exceed the elimination output.

These results were not evident from previous human exposure studies, because the target tissue disposition was not accurately determined (*17,18*). Utell et al. (*17*) exposed human volunteers to 129–137 mg D_4; the lungs only captured 10% of D_4 exposure by inhalation (13 mg out of 129–137 mg of inhaled D_4). Thus most of the inhaled dose (124 mg out of 137 mg) was not absorbed, which is expected from a combination of poor gas mixing in the lung, and alveolar tissue mass transfer resistance to hydrophobic materials such as D_4 because of the aqueous nature of the alveolar membrane. Utell et al. (*17*) reported that D_4 was rapidly cleared from plasma, but they did not identify D_4 tissues distribution or excretion as predicted by our model. Our PBPK model did confirm the plasma measurements reported by Utell et al. (*17*) as well as a nonlinear clearance with two half-lives of 30 min and 330 min and a mean peak value of 79 ng/g (Table 7 and Figure 6).

The pharmacokinetic results shown in Tables 5 and 7 for rats and humans, respectively, showed a disproportionate increase in area under the curve and volume of distribution at high dose and repeated exposures of D_4. The predicted D_4 plasma and fat behavior are similar to that observed with other volatile lipophilic chemicals such as styrene (*12,20*). Because the exposure was repeated daily, the D_4 concentrations in fat increased, as shown in Table 6. However, systemic clearance remained about the same regardless of the route of exposure (Table 7). The shape of the plasma and fat concentration–time curves shown in Figures 3–5 also suggested probable saturation of the elimination processes. On repeated dosing, saturation of the elimination processes may increase the delivered dose of D_4 to target organs such as fat, richly perfused tissues (e.g., lungs, brain), liver, and kidneys in both rats (Table 4) and humans (Table 6). In the liver and kidneys, such accumulation could produce liver enlargement confirming experimental results found in mice and rats (*1,13,15*). McKim et al. (*15*) reported some preliminary results suggesting that repeated inhalation exposure to high concentrations of D_4 produced liver enlargement with significant induction of cytochrome P_{450} CYP2B1/2 in rats. Analysis of the rat excretion results (Table 4) showed no compelling evidence of D_4 CYP enzyme induction. Furthermore, there is a more reliable way (e.g., using yeast that contains human genes) to determine whether D_4 chemically induced P_{450} in humans.

Table 6. Comparison of D_4 tissue distribution results in rats and humans as a percentage of doses. Rat experimental values in parentheses.

Tissue compartment	Rat IV[a] (7 mg/kg)	Human inhalation single exposure[b] (11.1 mg)	Human inhalation exposure, repeated[c] (77.7 mg)	Human breast implant exposure (10.4 mg)[d]
Richly perfused tissue	0.83	7.9	2.2	1.7
Fat	18.2 (16.3)	39.7	35.0	27.6
Liver	0.10 (0.15)	0.14	0.04	0.04
GI tract	0.001	0.005	0.001	0.002
Kidneys	0.04 (0.07)	0.14	0.04	0.04
Blood	0.15	0.08	0.01	0.01
Urine	26.1 (22.3)	6.1	7.3	8.6
Feces	8.71 (5.93)	2.0	2.4	2.9
Exhaled	42.2 (31.8)	43.8	53.1	59.1

[a]At the end of 48 hr. [b]At the end of 24 hr. [c]At the end of 7 days. [d]At the end of 7 days.

Table 7. Pharmacokinetic results of D_4 in human plasma.

Pharmacokinetic parameters	Human inhalation exposure (11.1 mg)	Human inhalation exposure, 7-day repeated dose (77.7 mg)	Human breast implant exposure[a] (10.4 mg)
C_{max} (ng/mL)	69.4	76.0	2.0
t_{max} (hr)	1	145	35
AUC (ng/hr/mL)	453.4	3,628	427.8
Cl (mL/hr)	407	357	329
V_d (L)	159.8	1,022	4,100
$t_{1/2}$ (hr)	1.7, 7.4[b]	1.1, 8.5[b]	7.8

Abbreviations: AUC, area under the curve of D_4 concentration in plasma versus time; Clearance (Cl), total body clearance; C_{max}, maximum concentration in plasma; t_{max}, maximum time; $t_{1/2}$, the elimination half life of D_4 in plasma; V_d , volume of distribution.
[a]81.4% of this dose of D_4 desorbed into the body at the end of 14 days. [b]Biphasic half-life.

The model predicted 43% and 53% of the dose of D_4 in exhaled air after single and repeated inhalation exposures, respectively. Similarly, 59% of D_4 was exhaled in air after breast implantation (Table 6). The model results were comparable with the exhalation data reported by others (*1,3,12,15,17*). The PBPK model used the blood:air partition coefficient to estimate the exhalation data of D_4. The blood:air partition coefficient that best fit the experimental data [shown in Table 3 as H_{air} (20.0)], was not consistent with the water:air partition coefficient values for D_4. The published Henry's law constants for D_4 (air:water) have been reported in the range of 3–32, which is equivalent to water:air partition coefficient of 0.33 to 0.031 (*27,29–32*). The discrepancy was attributed to both the low solubility of D_4 in water (56 ppb) and its binding to blood lipoproteins, which increased the value of the blood:air partition coefficient relative to its corresponding water:air partition coefficient (*33*). Beliveau and Krishnan (*33*) indicated that the blood:air partition coefficients of lipophilic volatile organic compounds (e.g., D_4, styrene) could not be determined using water:air partition coefficients. They published a methodology to account for this solubility enhancement of protein binding for estimating the blood:air partition coefficients using oil:water and *n*-octanol:hemoglobin:water mixtures instead of a simple water:air measurements (*33*). The high lipid affinity of D_4 for blood proteins makes this effect even more significant for this case. We suspected that a smaller blood:air partition coefficient (< 20) was used in a reported model by Anderson et al. (*16*). This could have led the authors to underestimate the postexposure blood and tissues levels of D_4 in rat (*16*).

We developed a PBPK model to determine the time course of D_4 in the human body after exposure at different doses and routes in rats and humans. The simulation results suggest that D_4's unique physicochemical properties play an important role in the bioavailability of this chemical. It is absorbed rapidly and retained in the fatty tissues for a longer time when it contacts lipophilic tissues directly (e.g., breast implants). The repeated daily inhalation exposures to D_4 would accumulate this compound in fat, liver, and kidneys significantly to saturate its elimination processes. This accumulation is likely to occur in women because physiologically women have a large volume of adipose tissues and a slower metabolism than do men. Future studies are expected to extend our toxicokinetic evaluation of D_4 such that we could accurately assess the safety of D_4 based on its bioavailability and target doses, not by consideration of the dose level alone.

Appendix

The material balances for both D_4 and its metabolites for the model shown in Figure 2 were solved using MathCad 8.0 (MathSoft, Inc., Cambridge, MA, USA). We used an adaptive grid Runge-Kutta method for the system of stiff ordinary differential equations. We calibrated the rat model using an IV dose; this was introduced as a forcing function partitioned to all of the compartments in the model. In that way, the D_4 was distributed to all compartments in the body, allowing the numerical procedure to converge to a solution. In the human inhalation or breast implant case, the D_4 was introduced directly to the lung or into the systemic circulation at the mix point, similar to previous models (*12,13*). A nomenclature list is included at the end of this appendix. The following equations are the material balances for D_4:

For the lung, $$V_{lung}\frac{dC_{lung}}{dt} = Q_tC_{ai} - Q_tC_{lung}H_{air}C_{lung}$$

For the richly perfused tissues, $$V_r\frac{dC_r}{dt} = Q_rC_{lung}H_{air} + \frac{Q_r\xi(t)}{Q_t} - \frac{Q_rC_r}{D_r}$$

For the deep fat compartment, $$V_{f2}\frac{dC_{f2}}{dt} = \frac{Q_{f2}C_{f2}}{D_{f2}} - \frac{Q_{f2}C_{f2}}{D_{f2}}$$

For the weakly bound fat compartment,

$$V_{f1}\frac{dC_{f1}}{dt} = Q_{f1}C_{lung}H_{air} + \frac{Q_{f1}\xi(t)}{Q_t} + \frac{Q_{f2}C_{f2}}{D_{f2}} - \frac{Q_{f1}C_{f1}}{D_{f1}} - \frac{Q_{f2}C_{f1}}{D_{f1}}$$

For the liver, $$V_l\frac{dC_l}{dt} = Q_lC_{lung}H_{air} + \frac{Q_l\xi(t)}{Q_t} - \frac{Q_lC_l}{D_r} - k_{el}C_l$$

For the GI tract, $$V_{gi}\frac{dC_{gi}}{dt} = Q_lC_{lung}H_{air} + \frac{Q_{gi}\xi(t)}{Q_t} - \frac{Q_{gi}C_{gi}}{D_{gi}}$$

For the kidneys, $$V_k\frac{dC_k}{dt} = Q_kC_{lung}H_{air} + \frac{Q_k\xi(t)}{Q_t} - \frac{Q_kC_k}{D_k}$$

We determined the total metabolites generated by integrating the accumulation equation below,

$$\frac{dM_{metabolite}}{dt} = k_{el}C_l$$

In the blood, D_4 exists dissolved in the plasma (aqueous), weakly bound to protein, and strongly bound to protein. The venous blood is well mixed before it is returned to the arterial circulation. At this mix point, the D_4 protein binding is calculated. For D_4 in the plasma,

$$V_{blood}\frac{dC_{ai}}{dt} = \frac{Q_rC_r}{D_r} + \frac{Q_{f1}C_{f1}}{D_{f1}} + \frac{Q_lC_l}{D_l} + \frac{Q_{gi}C_{gi}}{D_{gi}} + \frac{Q_kC_k}{D_k} + k_{wo}C_{wk} - k_{wi}C_{ai} - Q_tC_{ai}$$

For the weakly bound D_4 in the blood, $$V_{strong}\frac{dC_{str}}{dt} = k_{si}C_{wk} - k_{so}C_{str}$$

For the strongly bound D_4 in the blood,

Appendix 1, Table 1. Nomenclature.

C_{ai}	Concentration of D_4 dissolved in plasma, mol/mL
C_{air}	Concentration of D_4 in inhalation air, mol/L
C_{f1}	Concentration of D_4 in weakly bound fat compartment, mol/mL
C_{f2}	Concentration of D_4 in strongly bound fat compartment, mol/mL
C_{gi}	Concentration of D_4 in GI tract, mol/mL
C_k	Concentration of D_4 in kidneys, mol/mL
C_{inj}	Concentration of D_4 in IV fluid, mol/mL
C_r	Concentration of D_4 in richly perfused tissue, mol/mL
C_{wk}	Concentration of D_4 weakly protein bound in plasma, mol/mL
C_{str}	Concentration of D_4 strongly protein bound in plasma, mol/mL
D_0	Available dose of D_4 in breast implant shell, mol
D_{f1}	Distribution coefficient of D_4 in weakly bound fat compartment, dimensionless
D_{f2}	Distribution coefficient of D_4 in strongly bound fat compartment, dimensionless
D_{gi}	Distribution coefficient of D_4 in GI tract, dimensionless
D_k	Distribution coefficient of D_4 in kidney, dimensionless
D_l	Distribution coefficient of D_4 in liver, dimensionless
D_r	Distribution coefficient of D_4 in richly perfused tissue, dimensionless
H_{air}	Blood:air partition constant of D_4 in plasma, dimensionless
k_{ba}	Desorption constant of D_4 from breast implant shell, h^{-1}
k_{si}	Forward rate constant for strong protein binding of D_4 in plasma, h^{-1}
k_{el}	Metabolism rate constant, h^{-1}
k_{so}	Reverse rate constant for strong protein binding of D_4 in plasma, h^{-1}
k_{wi}	Forward rate constant for weak protein binding of D_4 in plasma, h^{-1}
k_{wo}	Reverse rate constant for weak protein binding of D_4 in plasma, h^{-1}
Q_{air}	Lung ventilation rate, L/hr
$Q_{exercise}$	Lung ventilation rate during exercise, L/hr
Q_{rest}	Lung ventilation rate during rest, L/hr
Q_{f1}	Blood flow rate to weakly bound fat compartment, mL/hr
Q_{f2}	Blood flow rate to strongly bound fat compartment, mL/hr
Q_{gi}	Blood flow rate to GI tract, mL/hr
Q_{inj}	Flow rate of IV, mL/hr
Q_k	Blood flow rate to kidneys, mL/hr
Q_l	Blood flow rate to liver, mL/hr
Q_r	Blood flow rate to richly perfused tissues, mL/hr
Q_t	Total cardiac output, mL/hr
t	Time, hr
t_{inj}	Duration of IV, hr
V_{blood}	Plasma volume, mL
V_{f1}	Volume of weakly bound fat compartment, mL
V_{f2}	Volume of strongly bound fat compartment, mL
V_{gi}	Volume of GI tract, mL
V_k	Volume of kidneys, mL
V_l	Volume of liver, mL
V_{lung}	Volume of lungs, mL
V_r	Volume of richly perfused tissue, mL
V_{strong}	Volume of strongly bound plasma, mL
V_{weak}	Volume of weakly bound plasma, mL

$$V_{weak}\frac{dC_{wk}}{dt} = k_{wi}C_{ai} + k_{so}C_{str} - k_{wo}C_{wk} - k_{si}C_{str}$$

For the IV case in the rat, we solved the above equations with the initial conditions that all the compartments except the weakly bound D_4 in the blood have zero concentration at $t = 0$. The weakly bound D_4 in the blood was assigned an initial concentration of D_4 equal to 5% of the IV dose at $t = 0$; this was a better fit of the experimental data.

For the rat, the IV dose was input using the following forcing function. $$\xi(t) = \text{if}(t < t_{inj}, Q_{inj}C_{inj}, 0)$$

For the human, the IV dose was replaced by either an inhalation dose or implant dose. Using the data of Utell et al. (*11*), we exposed subjects to 10 ppm D_4 by inhalation for 1 hr. This exposure period consisted of 10 min rest, 10 min exercise, 20 min rest, 10 min exercise, and finally 10 min rest before the D_4 inhalation was terminated.

To model this, we defined five forcing functions covering each period of exposure. The inhalation rate was set at 10 L/min during rest, and 30 L/min during exercise. Using Utell et al.'s (*11*) published capture efficiencies of the human lung of 0.12 during rest and 0.07 during exercise, we delivered a total dose of 11.1 mg of D_4 to the human body during the exposure. The following equations were used,

$$\chi_1(t) = \text{if}(t < 10\ \text{min}, Q_{rest}C_{in}, 0)$$

$$\chi_2(t) = \text{if}(10 \le t < 20\ \text{min}, Q_{exercise}C_{in}, 0)$$

$$\chi_3(t) = \text{if}(20 \le t < 40\ \text{min}, Q_{rest}C_{in}, 0)$$

$$\chi_4(t) = \text{if}(40 \le t < 50\ \text{min}, Q_{exercise}C_{in}, 0)$$

$$\chi_5(t) = \text{if}(50 \le t < 60\ \text{min}, Q_{rest}C_{in}, 0)$$

During the exposure, Q_{air} in equation 1 is also stepped between Q_{rest} and $Q_{exercise}$ during the 1-hr exposure. After exposure, the lung ventilation rate was set to the resting value. In the human case, unlike the rat, all of the compartments contained no D_4 at t = 0. Also, unlike the rat where 5% of the D_4 was initially bound to the blood plasma, in the human this value was set to 0.8% of the dose delivered by the functions

$$\chi 1(t) - \chi 5(t).$$

For the human breast implant exposure, the inhalation forcing functions were replaced by a first-order desorption.

$$k_{ba}D_0 exp(-k_{ba}t)$$

References and Notes

1. Kirkpatrick D. ^{14}C-D_4 Pharmacokinetics in the Rat Following Intravenous Administration. Huntington Research Center Ltd. Sponsored by Silicone Environment Health and Safety Council. Midland, MI:Dow Corning Corporation, 1995.
2. Modler RF. Cosmetic chemicals. Specialty Chemicals Update Program, Vol 6. Menlo Park, CA:SRI International, 1992;65.
3. Shields HC, Fleischer DM, Weschler CJ. Comparisons among VOCs measured in three types of commercial buildings with different occupant densities. Indoor Air 6:2–17 (1996).
4. Shipp AM, Van Landingham CV, Meeks RG. Estimation of margins of exposure: a preliminary risk assessment for octamethylcyclosiloxane (D_4) based on reproductive toxicity studies in Sprague-Dawley rats. [Abstract] Toxicologist 54(1):108 (2000).
5. Compton RA. Silicone manufacturing for long-term implants. J Long Term Effects of Med Implants 7(1):29–54 (1997).
6. Carmichael JB, Winger R. Cyclic distribution in dimethylsiloxanes. J Polym Sci Part A 3:971–981 (1965).
7. Sun LF, Alexander H, Lattarulo N, Blumenthal NC, Ricci JL, Chen GG. Protein denaturation induced by cyclic silicone. Biomaterials 18(24):1593–1597 (1997).
8. Yu LT, Lamore G, Marotta J, Batich C, Hardt NS. *In vitro* measurements of silicone bleed from breast implants. Plast Reconstr Surg 97(4):756–764 (1996).
9. Lykissa ED, Kala SV, Hurley JB, Lebovitz RM. Release of low molecular weight silicones and platinum from silicone breast implants. Anal Chem 69:4912–4916 (1997).
10. Garrido L, Pfleiderer B, Jenkins BG, Hulka CA, Kopans DB. Migration and chemical modification of silicone in women with breast prostheses. Magn Reson Med 31:328–330 (1994).
11. Pfleiderer B, Garrido L. Migration and accumulation of silicone in the liver of women with silicone gel-filled breast implants. Magn Reson Med 33:8–17 (1995).
12. Plotzke KP, Crofoot SD, Ferdinandi ES, Beattie JG, Reitz RH, McNett DA, Meeks RG. Disposition of radioactivity in Fischer 344 rats after single and multiple inhalation exposure to ^{14}C octamethylcyclotetrasiloxane D_4. Drug Metab Dispos 28:192–204 (2000).
13. Lieberman MW, Lykissa ED, Barios R, Ou CN, Kala G, Kala SV. Cyclosiloxanes produce fatal liver and lung damage in mice. Environ Health Perspect 107(2):161–165 (1999).
14. Kala SV, Lykissa ED, Neely MW, Lieberman MW. Low molecular weight silicones are widely distributed after a single subcutaneous injection in mice. Am J Pathol 152(3):645–649 (1998).
15. McKim JM Jr, Kolesar GB, Dochterman LW, Wilga PC, Hubbell BG, Mast RW, Meeks RG. Effects of octamethylcyclotetrasiloxane (D_4) on liver size and cytochrome P450 in Fisher rats: a 28 day whole body inhalation study [Abstract]. Toxicologist 15(1):117 (1995).
16. Andersen ME, Sarangapani R, Reitz RH, Gallavan RH, Plotzke KP. Pharmacokinetic modeling of octamethylcyolotetrasiloxane (D_4) in rats: single and repeat inhalation exposure. [Abstract] Toxicologist 48(1):143 (1999).
17. Utell MJ, Gelein R, Yu CP, Kenaga C. Geigel E, Torres A, Chalupa D, Gibb FR, Speers DM, Mast RE, et al. Quantitative exposure of humans to an octamethylcyoctotetrasiloxane (D_4) vapor. Toxicol Sci 44:206–213 (1998).
18. Looney RJ, Frampton MW, Byam J, Kenaga C, Speers DM, Cox C, Mast R, Klykken PC, Morrow PE, Utell MJ. Acute respiratory exposure of human volunteers to octamethylcyclotetrasiloxane (D_4): absence of immunological effects. Toxicol Sci 44:214–220 (1998).
19. Ramsey JR, Anderson ME. A physiologically based description of the inhalation pharmacokinetics of styrene in rats and humans. Toxicol Appl Pharmacol 73:159–175 (1984).
20. Luu HMD, Hutter JC. Pharmacokinetic modeling of 4,4′-methylenedianiline released from reused polyurethane dialyzer potting materials. J Biomed Mater Res (Appl Biomater) 53:276–286 (2000).
21. Varaprath S, Salyers KL, Plotzke KP, Nanavati S. Extraction of octamethylcyclotetrasiloxane and its metabolites from biological matrices. Anal Biochem 256:14–22 (1998).
22. McGilvery RW. Biochemistry, A Functional Approach. 2nd ed. Philadelphia, PA:W.B. Saunders Company, 1979.
23. Krishnan K, Andersen ME. Physiologically based pharmacokinetic modeling in toxicology. In: Principles and Methods of Toxicology (Hayes AW, ed). 3rd ed. New York:Raven Press, 1994;149–188.
24. Favre E, Schaetzel P, Nguyen QT, Clement R, Neel J. Sorption, diffusion and vapor permeation of various penetrants through dense poly(dimethylsiloxane) membranes: a transport analysis. J Membr Sci 92:169–184 (1994).
25. Zielinski JM, Duda JL. Predicting polymer/solvent diffusion coefficients using free volume theory. AIChE J 38(3):405–415 (1992).
26. Crank J. The Mathematics of Diffusion. New York:Oxford University Press, 1975.
27. Lichtenthaler RN, De Azevedo EG, Prausnitz JM. Molecular Thermodynamics of Fluid Phase Equilibria. 3rd ed. New York:Prentice Hall, Inc., 1998.
28. Jovanovic ML, McMahon JM, McNett DA, Tobin JM, Gallavan RH Jr, Plotzke KP. In vivo percutaneous absorption of ^{14}C-Octamethylcyclotetrasiloxane in Fisher 344 rats. [Abstract] Toxicologist 54(1):148 (2000).
29. Hamelink JL, Simon PB, Silberhorn EM. Henry's law constant, volatization rate, and aquatic half life of octamethylcyclotetrasiloxane. Environ Sci Technol 30 (6):1946–1952 (1996).
30. Kent DJ, McNamara PC, Putt AE, Hobson JF, Silberhorn EM. Octamethylcyclotetrasiloxane in aquatic sediments: toxicity and risk assessment. Ecotox Environ Saf 29:372–389 (1994).
31. Hobson JF. Existing chemical testing for environmental fate and effects under TSCA section 4: a case study with octamethylcyclotetrasiloxane (OMCTS). Environ Toxicol Chem 14:1635–1638 (1995).
32. Perry RH, Green DW, Maloney JO, eds. Perry's Chemical Engineer's Handbook. 6th ed. New York:McGraw-Hill Book Company, 1984;4–60.
33. Beliveau M, Krishnan K. Estimation of rat blood: air partition coefficients of volatile organic chemicals using reconstituted mixtures of blood components. Toxicol Lett 116:183–188 (2000).